VOL. 5, NO. 3, MARCH 2010 ISSN 1819-6608
ARPN Journal of Engineering and Applied Sciences

www.arpnjournals.com

COMPONENT MODEL-BASED CONDITION MONITORING OF A GAS TURBINE

E. A. Ogbonnaya[1], K. T. Johnson[1], H. U. Ugwu[2] and C. U. Orji[1]
[1]Department of Marine Engineering, Rivers State University of Science and Technology, Port Harcourt, Nigeria
[2]Department of Mechanical Engineering, Michael Okpara University of Agriculture, Umudike-Umuahia, Nigeria
E-Mail: ezenwaogbonnaya@yahoo.com

ABSTRACT

In recent years, the requirements for reliability of machines that perform different technological processes and their faults diagnoses have become much stricter on most plants. The individual component models are used to generate the source or cause of fault in the engines. The failure of these components poses a great problem to the equipment manufacturers and owners. A step to the reduction of the faults led to the execution of this work using gas turbine engines as case studies. Component parametric readings collected from a gas turbine engine on industrial duty for power generation were used to enunciate steps to solve the problem by simulating likely deterioration in its component data. A computer program code in Visual Basic was used to actualize the simulation. The results obtained show that early detection of faults could help to avoid catastrophic downtime. Also the research revealed that the pressure drop across turbine should not exceed 11.4 bar for optimum performance.

Keywords: model, gas turbine, component parametric model, pressure ratio, boost pressure, compressor, turbine isentropic efficiency.

INTRODUCTION

The gas turbine (GT) is a complex installation and requires high reliability and availability for the safe output delivery. Therefore, there is need for the improvement in engine reliability and consequent reduction in maintenance cost can be met through effective and continual condition and health monitoring of the engine.

Component modeling is the systematic diagnostic field test procedures and computer analysis of individual components usually needed to define exact causes and optimum solution of faults. Component modeling therefore reduces the difficulty of diagnosing the malfunctions of the engine for the smooth running (Bergman, *et al*, 1993).

According to Ogbonnaya (1998) as shown in Figure-1, Component models are thus used to generate output variables for the effective and efficient health monitoring of the engine. This is in case the system variable exceeds unacceptable limits. They also help to detect imminent failures before limits are exceeded and equally assist to predict the time when failures become critical.

Furthermore, component models give recommendation for operation and maintenance thereby reducing systems cost and promoting its reliability (Bergman, *et al*, 1993). The application of component models in monitoring systems therefore offers good possibility in describing the relation between the component input and output variables on real time online basis (Stanatis, *et al*, 2001).

The simplest form of the model consists of a set of formulae, obtained by curve fitting using test-bed data or commissioning measurements. During the measurement, the particular component must be in a healthy condition as shown in Figure-1. It is also important that the monitoring system use the same sensor as was used for the determination of the reference model.

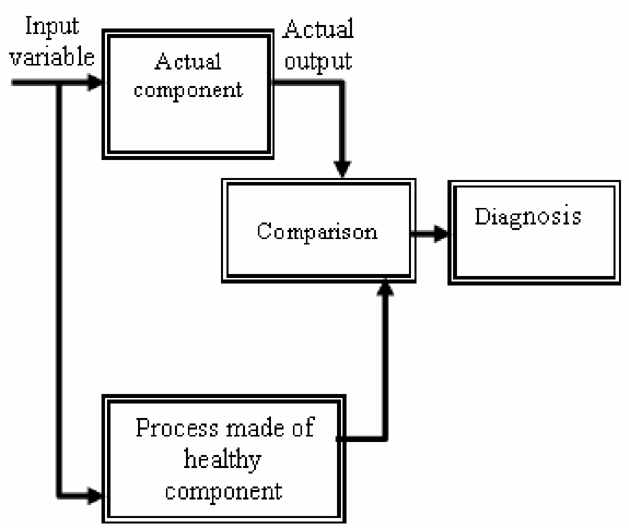

Figure-1. Component model for monitoring and diagnosis.

This other type of application comes into use, as the system being modeled gets more complex. The general component structure that can be used to come up with this model in this case is shown in Figure-2.

The physical process enables the creation of model, which is more generally applicable. It is therefore sensible to develop a model, which consists of physical relation and is tuned to the actual engine on the basis of few measurements (Baker, 1991).

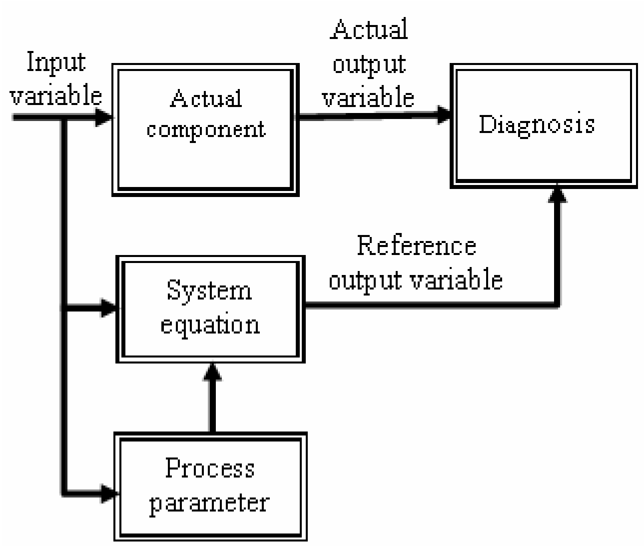

Figure-2. General component structure.

The application of a component model for a particular engine component is limited by physical knowledge through its source as a good example to illustrate the general model structure. The model enables detection of malfunction of the component by means of comparing the relationship between actual and reference output (Ogbonnaya, 1998).

According to Alexious and Mathioudakis (2006), there is need to achieve real time engine condition monitoring and prediction of real time engine health prognostics. This enhances maintenance process by enabling reduction in maintenance staff hours, improvements in diagnostic performance, increasing readiness and providing the information required to optimize maintenance scheduling based on need and current research and development aimed at finding a proof of concept.

MATERIALS AND METHODS

The GT engine is a complex installation. Its processes represent all the interaction imposed onto its components by the fact that they are linked to form the GT plant. So, it became necessary to monitor the individual components of a GT so that the complete unit will give the required performance without abnormality when running at the designed point (Aretakis *et al.*, 2002).

Some components of the GT machine considered in the course of this work are as follows:

- The compressor
- The turbine
- The combustion

The compressor

The compressor is one of the major components of a GT power plant and was given greater attention when thinking of monitoring the condition of the GT engine. The GT compressor is of two major types-namely:

a) The axial compressor.

b) The centrifugal compressor.

For the purpose of this paper, the centrifugal compressor, used in Afam 19 and 20 GT power plants was considered (Afam GT manual, 2001). This is usual for marine application also. The monitoring of the compressor involved a number of mechanical alterations to simulate faults on the component. They included the insertion of an inlet obstruction, an obstruction in a diffuser passage, variation of impeller tip clearance to reduce fouling. Two other kinds of measurements normally required for the condition monitoring of the compressor of the GT engine are sound emission and casing vibration (Azovtsev and Barkov, 1988). These are however outside the scope of this paper.

In this work, the major parameters considered for monitoring the GT compressor are pressure ratio also known as boost pressure, area/mass flow of air, speed of the linking shaft of the compressor to the turbine (Ogbonnaya, 2004), compressor outlet temperature and compressor efficiency.

Likewise the performance of the compressor was monitored using the following formulae:

$$\Delta T_{12} = \frac{T_1}{\eta_c}\left[\left(\frac{P_2}{P_1}\right)^{\frac{\gamma-1}{\gamma}} - 1\right] \quad (1)$$

i.e.

$$T_2 - T_1 = \frac{T_1}{\eta_c}\left[\left(\frac{P_2}{P_1}\right)^{\frac{\gamma-1}{\gamma}} - 1\right] \quad (2)$$

$$\eta_c = \frac{\left(\frac{P_2}{P_1}\right)^{\frac{\gamma-1}{\gamma}} - 1}{\left[\frac{T_2}{T_1} - 1\right]} \quad (3)$$

Where

ΔT_{12} = Temperature rise across the compressor

T_1 = Air Inlet temperature to the compressor

T_2 = Outlet temperature from the compressor

η_c = Isentropic efficiency of the compressor (IEC)

P_1 = Compressor inlet pressure

P_2 = Compressor outlet pressure

γ = Isentropic compression constant (ratio of specific heats)

Equation (3) was used to write the program for monitoring the compressor health condition.

The turbine

ARPN Journal of Engineering and Applied Sciences

www.arpnjournals.com

The turbine is another major component of a GT engine whose deterioration or degradation in service is detrimental to the maintenance personnel and also requires an efficient diagnostic system to provide detailed diagnostic information with the highest possible reliability. In this component, the fault diagnosis was directed towards finding the deterioration in temperature across the turbine, which could be mathematically written as:

$$\Delta T_{34} = \eta_T \ T_3 \left[1 - \left(\frac{1}{\frac{P_3}{P_4}} \right)^{(\gamma-1)/\gamma} \right] \quad (4)$$

Where

$$P_3 / P_4 = r_p$$

$$\therefore \quad \Delta T_{34} = \eta_T T_3 \left[1 - \left(\frac{1}{r_p} \right)^{\frac{\gamma-1}{\gamma}} \right] \quad (5)$$

$$If \quad \Delta T_{34} = T_3 - T_4 \ ,$$

$$Then \quad T_3 - T_4 = \eta_T T_3 \left[1 - \left(\frac{1}{r_p} \right)^{\frac{\gamma-1}{\gamma}} \right] \quad (6)$$

$$\eta_T = \frac{T_3 - T_4}{T_3 \left[1 - \left(\frac{1}{r_p} \right)^{\frac{\gamma-1}{\gamma}} \right]} \quad (7)$$

Where

ΔT_{34} = temperature difference between inlet to the turbine and the outlet from the turbine
η_t = turbine isentropic efficiency (IET)
T_3 = inlet temperature of gas to the turbine
P_3= inlet pressure of gas to the turbine
P_4 = outlet pressure of gas from the turbine
γ = isentropic expansion constant.

To calculate for Network output, combine equations (1) and (4), to get

$$W_{net} = M_g C p_g \Delta T_{34} - \frac{1}{\eta_m} M_a C p_a \Delta T_{12}$$

Where

$W_{net} = W_t - W_c$ and

$$W_t = Cp_g M_g \ (T_3 - T_4) \quad (8)$$

$$W_c = Cp_a M_a \ (T_2 - T_1) \quad (9)$$

then,

$$\eta_m = \frac{- M_a C p_a (T_2 - T_1)}{W_{net} - M_g C p_g \Delta (T_3 - T_4)}$$

Where

Cp_g = constant pressure specific heat capacity of gas
Cp_a = constant pressure specific heat capacity of air
W_{net} = Network
η_m = Mechanical efficiency
ΔT_{34} = Temperature differential between turbine inlet and outlet
(Klaus and Rainer, 2000; Kurzke, 2002)

The combustion chamber

Combustion in the normal open cycle GT is a continuous process in which fuel is burnt in the air supplied by the compressor. An electric spark is required only for initiating the combustion process. Thereafter the flame must be self-sustaining. For combustion systems, the latter implies the need for high combustion efficiency and low pressure losses. Typical values assumed for cycle calculations being 99 percent for combustion and 2-8 percent of the compressor delivery pressure for cooling. The effect of these losses on cycle efficiency and specific output is not so pronounced as that of inefficiencies in the turbo machinery. The combustor is a critical component because it must operate reliably at extreme temperature to provide a suitable temperature distribution at entry to the turbine (Cohen *et al.,* 1998).

Probably the only feature of the GT that give the combustor designers problem is the peculiar interdependence of the compressor delivery, air density and mass flow. This leads to the velocity of the air at entry to the combustion system being reasonably constant over the operating range. The GT cycle is very sensitive to component inefficiencies. It is therefore important that the aforementioned requirement be met without sacrificing combustion efficiency. That is, it is essential that over most of the operating range, all the fuel injected has to be completely burnt and the fuel calorific value realized. Any pressure drop between inlet and outlet of the combustor leads to both an increase in Specific Fuel Consumption and a reduction in specific power output. So it is essential to keep the pressure loss to a minimum.

This was calculated regarding the overall stagnation pressure loss as the sum of the fundamental loss (a small component which is a function T_2/T_1) and the friction loss mathematically, written as:

Pressure loss factor, *PLF* =

$$\frac{\Delta P_\upsilon}{m^3 / 2\rho_1 A_m^2} = K_1 + K_2 \left(\frac{T_2}{T_1} - 1 \right) \quad (10)$$

ARPN Journal of Engineering and Applied Sciences

www.arpnjournals.com

Note that rather than $\rho_1 \, C_1^2/2$, a conventional dynamic head is used based on a velocity calculated from the inlet density, air mass flow, m and maximum cross sectional area, Am of the chamber. Velocity, sometimes known as the reference velocity is more representative condition in the chamber, and the convention is useful when comparing results from chambers of different shapes while K1 and K2 were determined from a combustion chamber on a test rig from cold run and hot run, respectively. Equation (10) is illustrated in Figure-3.

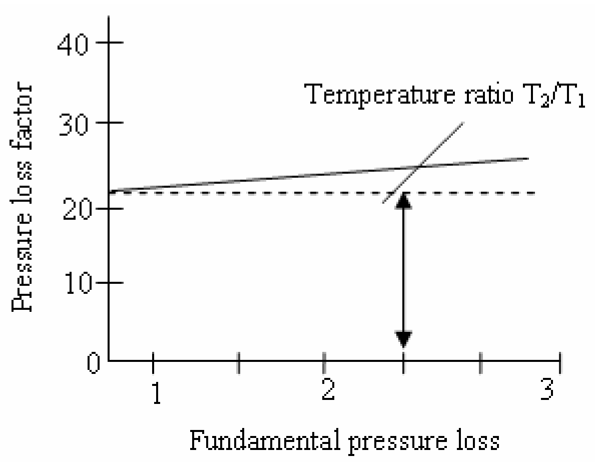

Figure-3. Variation of pressure loss factor with temperature ratio.

Then equation (10) enabled the pressure loss to be estimated when the chamber was operating as part of a GT over a wide range of condition of mass flow, pressure ratio and fuel input. Secondly, it should be appreciated from the viewpoint of cycle performance calculations that it is ΔP_v as a fraction of the compressor delivery pressure that is the useful parameter. This was related to the (PLF) as follows:

$$\frac{\Delta P_o}{P_1} = \frac{\Delta P_i}{m^2 / 2\rho_1 A_m^2} \times \frac{m^2 / 2\rho_1 A_m^2}{P_{01}} = PLF \times \frac{R}{2}\left(\frac{m\sqrt{T_1}}{A_m P_1}\right)^2 \qquad (11)$$

Where

Δp = pressure differential
m = mass flow rate
ρ = air density
A_m = maximum area
T_1 = inlet temperature
P_1 = inlet pressure
R = gas constant [Nag, 2005]

ANALYSIS AND DISCUSSION OF RESULTS

The results shown in Tables 1 and 2 were generated from a program code whose flowchart is shown in Figure-4. This flowchart was used to generate a computer program in visual basic. This single-loop flowchart is for the compressor, turbine performances, net power output and combination of all. The essence of presenting the flowchart and thus the program in that order was to make sure all the important parameters in the equation to write the program were captured in the monitoring of the engine. This is a novel introduction that will help to improve the performance of GTs. The Tables contain values of parameters obtained from operational GT19 and GT20 on industrial duty for electricity generation in Afam thermal power station in Port Harcourt, Nigeria. The design and manufacturing characteristics of the plants are shown in Appendix-1.

It is noteworthy that pressure loss across the turbine is equal to 11.4 bar. This shows that the results correspond with the manufacturer’s set standard. In the case where it is below the set standard, this could be attributed to long suction inlet duct of the compressor getting blocked. This gave the reduced pressure to the combustion chamber and also a higher pressure loss across the turbine.

Table-1. Program results obtained from GT UNIT 19.

IEC	T12	RPC	IET	T34	RPT	Wnet
0.455	319	9.64427	0.7846	469	9.51581	253767.45
0.4551	319.2	9.68379	0.7848	471	9.52571	254868.3
0.4558	319.8	9.72331	0.785	473	9.54547	255969.15
0.4565	320.4	9.76283	0.7852	475	9.56523	257070
0.4572	321	9.80235	0.7854	477	9.58499	258170.85
0.4579	321.6	9.84187	0.7856	479	9.60475	259271.7
0.4586	322.2	9.88139	0.7858	481	9.62451	260372.55
0.4593	322.8	9.92091	0.786	483	9.64427	261473.4
0.46	323.4	9.96043	0.7862	485	9.66403	262574.25
0.4607	324	9.99995	0.7864	487	9.68379	263675.1
0.4614	324.6	10.03947	0.7866	489	9.70355	264775.95
0.4621	325.2	10.07899	0.7868	485	9.72332	265876.8

Table-2. Program results obtained from GT UNIT 20.

IEC	T12	RPC	IET	T34	RPT	Wnet
0.4584	289.4	9.48617	0.7807	451	9.49605	251261.71
0.4595	292.6	9.49605	0.781	453	9.50593	251291.92
0.4606	295.8	9.50593	0.7813	455	9.51581	251322.13
0.4617	299	9.51581	0.7816	457	9.52569	251352.34
0.4628	302.2	9.52569	0.7819	459	9.53557	251382.55
0.4639	305.4	9.53557	0.7822	461	9.54545	251412.76
0.465	308.6	9.54545	0.7825	463	9.55533	251442.97
0.4661	311.8	9.55533	0.7828	465	9.56521	251473.18
0.4672	315	9.56521	0.7831	467	9.57509	251503.39
0.4683	318.2	9.57509	0.7834	469	9.58497	251533.6
0.4694	321.4	9.58497	0.7837	469	9.59485	251563.81
0.4705	324.6	9.59485	0.7837	469	9.60473	251594.02

ARPN Journal of Engineering and Applied Sciences

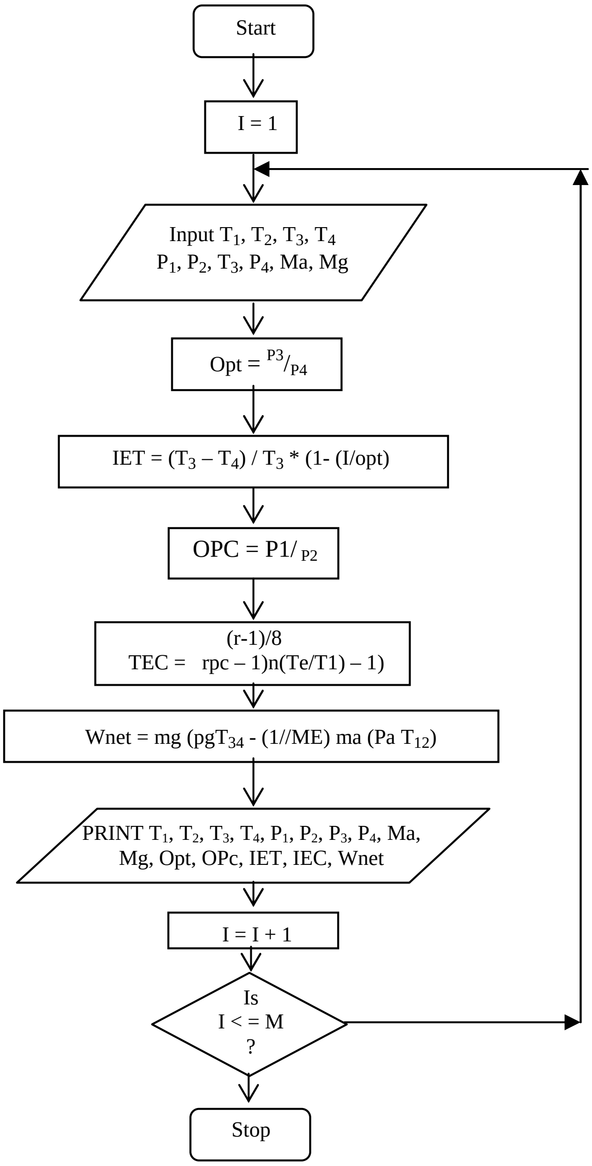

Figure-4. Flowchart for the computer code used to actualize the model.

From Table-1, the graphs shown on Figures 5 to 10 were plotted. Figure-5 is a graph of temperature rise against isentropic efficiency of the compressor. There is an increase in efficiency with gradual increase in temperature rise across the compressor from the point of 319 to 319.2oC of temperature rise after which corresponding increase in temperature brings about increase in efficiency. The above operational range is the brief region of transient analysis that should be avoided in the running of compressor.

Figure-6 shows the graph of pressure ratio of the compressor against the isentropic efficiency of the compressor. There was negligible increase of isentropic efficiency of the compressor with increase in pressure ratio from 9.644 to 9.684. This is another critical region to be avoided in the compressor operation as increase in pressure ratio is supposed to accompany increased isentropic efficiency.

Figure-7 is the graph of net power output against isentropic efficiency of the compressor of GT Unit 19. There is a corresponding increase in net power output with increase in efficiency of the compressor.

A region where increased isentropic efficiency does not attract a corresponding increase in net power output is to be avoided in the design and operation of GT compressors.

It is observed that a corresponding increase in temperature drop brings about corresponding increase in isentropic efficiency of the turbine until the point of maximum temperature drop across the turbine. This is shown in Figure-8. The implication is that a temperature drop of 483^{o}C and isentropic efficiency above 16.79% need to be avoided in the design and operations of turbines.

It is observed that corresponding increase in pressure ratio of the compressor tends to increase with the isentropic efficiency of the turbine until the maximum temperature drop is similar to that contained in Cohen *et al.*, (1998). Figure-9 shows the graph of pressure ratio against isentropic efficiency of turbine (GT 19).

Also, in Figure-10, it is observed that corresponding increase in efficiency attributes to the increase in net power output of the turbine to the maximum point.

From Figures 9 and 10, increased isentropic efficiency of turbines needs to be followed with increase in pressure ratio and net power output.

Figures 11 and 12 are the interface operational/performance displays for the compressors and turbines of GT 19 and 20, respectively. The salient feature of these Figures is that they provide continuous online routine assessment of the GT engine parametric performance. That is to say a change of one of the parameters will bring about a holistic change in the result of the entire system. This novel addition to GT condition monitoring equally means that fault on any component (turbine or compressor) that affect the others would be depicted on that interface immediately.

 ISSN 1819-6608

ARPN Journal of Engineering and Applied Sciences

www.arpnjournals.com

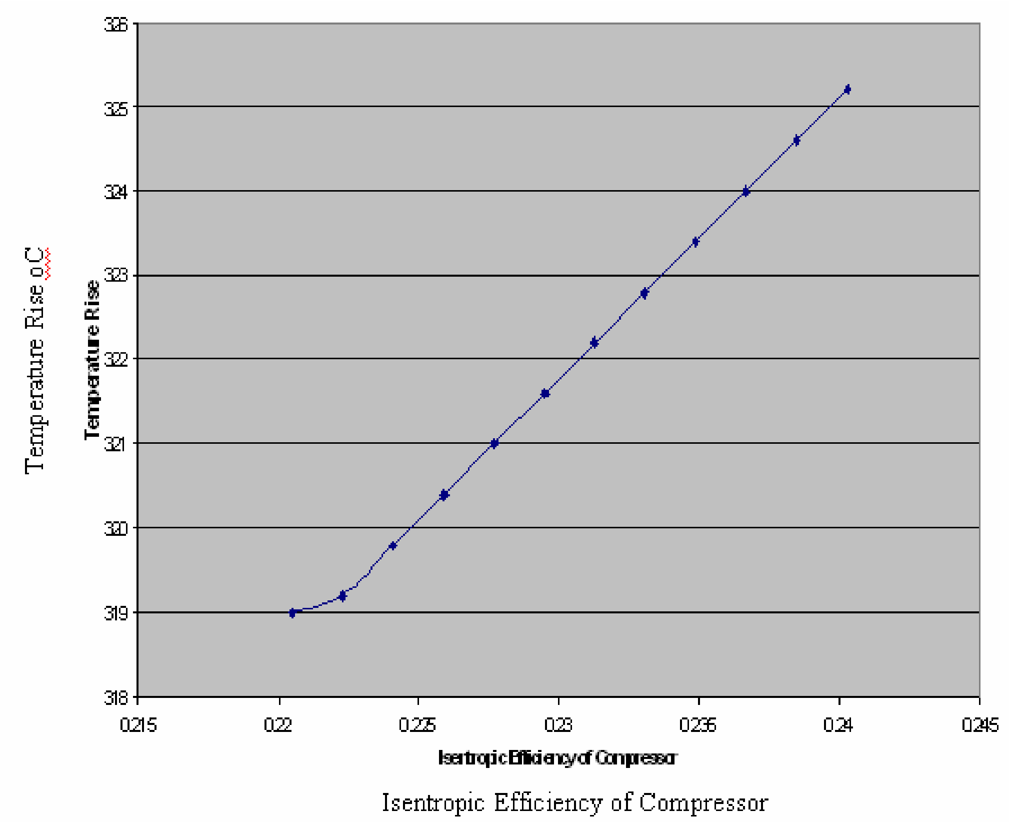

Figure-5. Temperature rise against isentropic efficiency of compressor (GT 19).

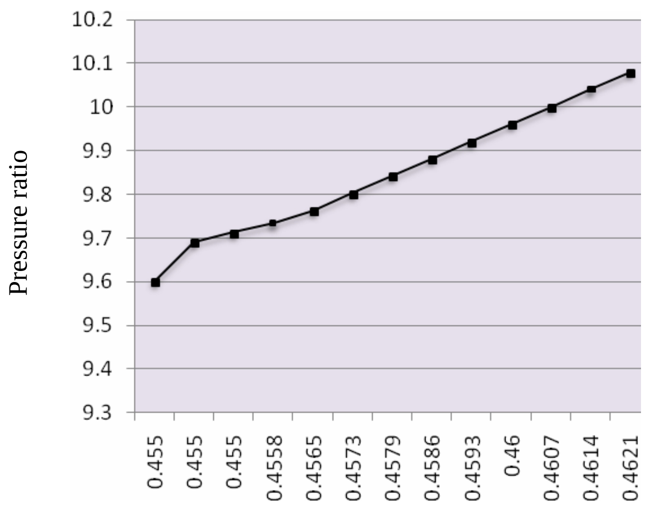

Isentropic efficiency of compressor

Figure-6. Pressure drop against isentropic efficiency of compressor (GT 19).

ARPN Journal of Engineering and Applied Sciences

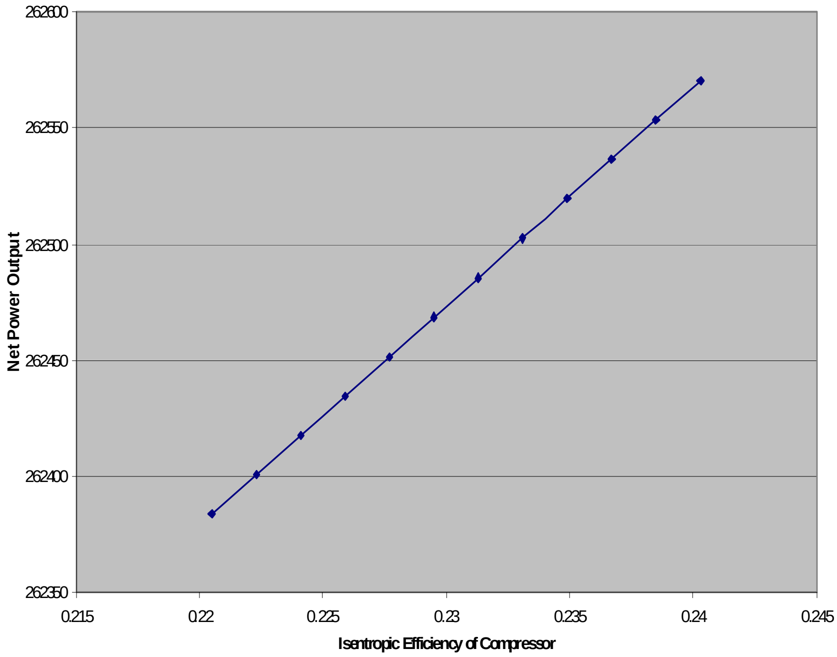

Figure-7. Net power output against isentropic efficiency of compressor (GT 19).

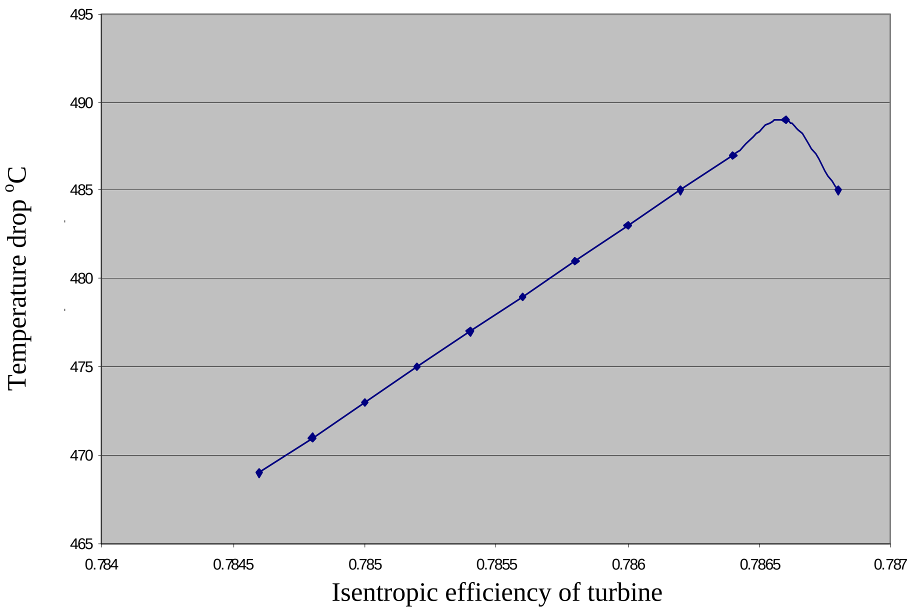

Figure-8. Temperature drop versus isentropic efficiency of turbine (GT 19).

VOL. 5, NO. 3, MARCH 2010 ISSN 1819-6608
ARPN Journal of Engineering and Applied Sciences

www.arpnjournals.com

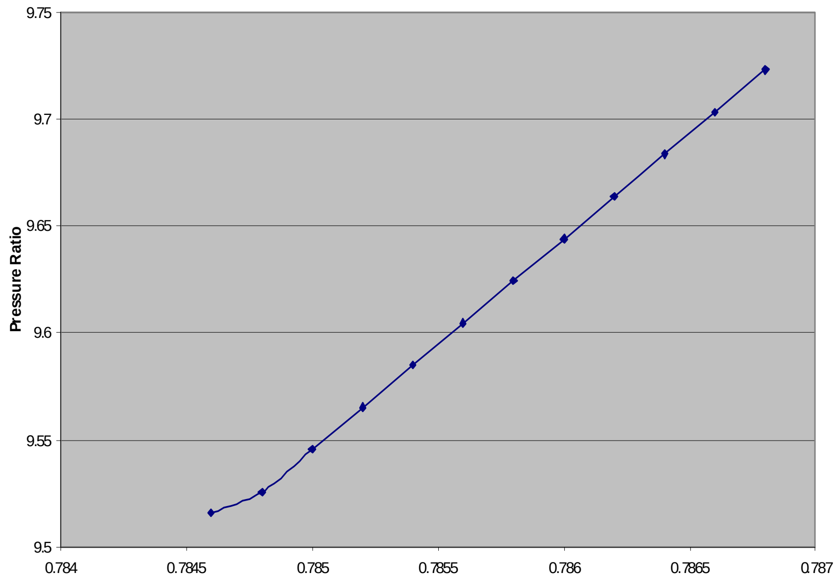

Isentropic efficiency of turbine

Figure-9. Pressure ratio against isentropic efficiency of turbine (GT 19).

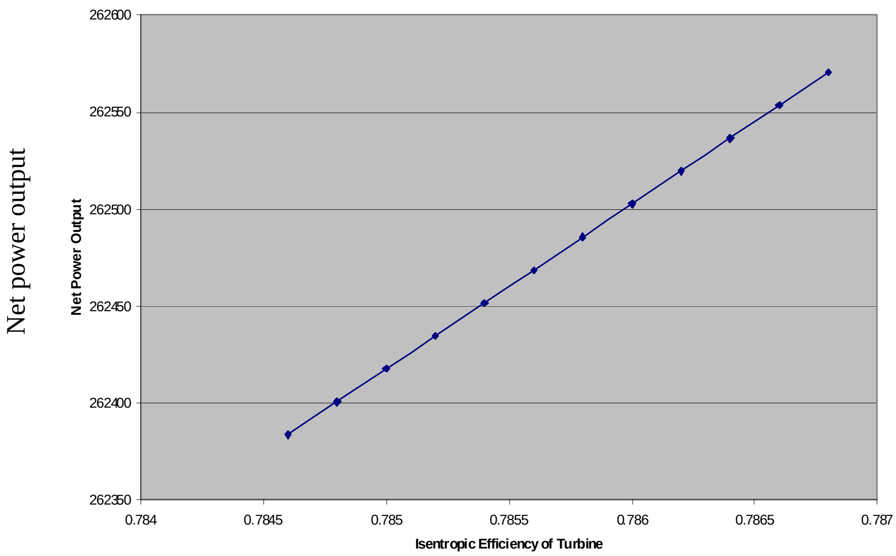

Isentropic efficiency of turbine

Figure-10. Net power against isentropic efficiency of turbine (GT 19).

CONCLUSIONS

A computer model for monitoring the operational parameters of GT compressor and turbine has been propounded through this work. The GT operational parameters looked at are the temperature, pressure, net power output, efficiencies and airflow rate.

There is efficient performance of the turbine at increased pressure ratios. This attributes to a high efficiency of the turbine and the health of a GT engine component can be predicted through its pressure drop across the turbine. The net power output of the turbine and compressor are solely dependent on the efficiency of the component. It was observed that the temperature rise across the compressor was a good attribute to the isentropic efficiency of the compressor.

Furthermore, it was noticed that beyond the maximum temperature drop across the turbine, efficiency became constant as pressure drop increased. A step-by-step analysis of the plant parameters obtained was used to develop a computer program to determine the condition of the components of the plant.

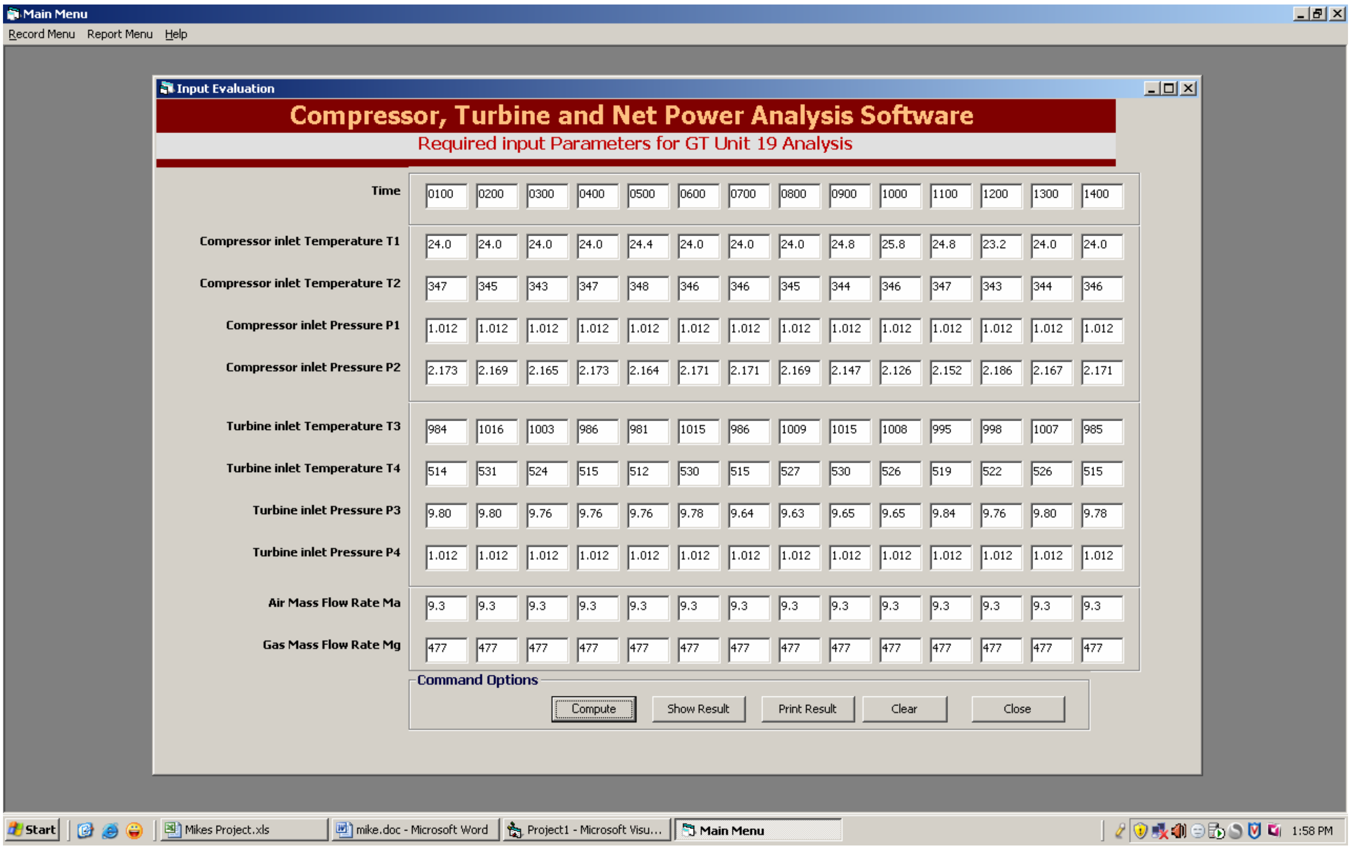

Figure-11. Input/out compressor and turbine operational display for GT unit 19.

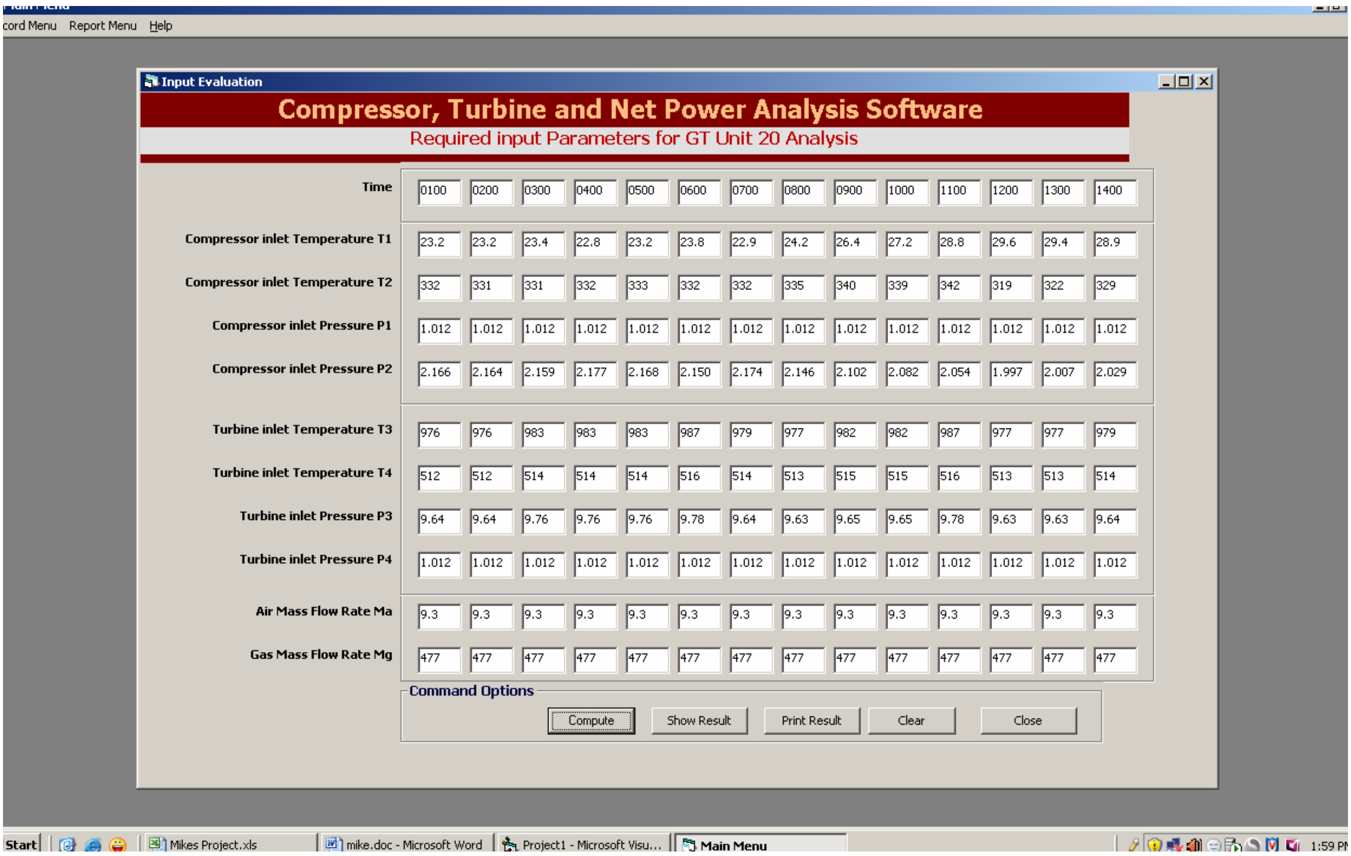

Figure-12. Input/out compressor and turbine operational display for GT unit 20.

RECOMMENDATIONS

Based on the results obtained in the course of this work, the following recommendations are hereby made:

a) High pressure ratio should be aimed at during design of GT plants;
b) There should be a set limit of maximum temperature drop during the design of GTs; and
c) High temperature rise across the compressor should be aimed at during the design of GT plants.

ACKNOWLEDGEMENTS

Our profound full-heart appreciation goes to Mr. Ovodo, Michael who took tireless time to go to Afam Thermal Station to carry out the experimentations that led to the actualization of this work. He equally produced the first manuscript and result for the work. We also thank the management and staff of the power station for allowing the use of GT19 and GT20 for the research.

REFERENCES

Alexious A. and Mathioudakis K. 2006. Gas Turbine Engine Performance Model Applications using an Objective Oriented Simulation Tool. American Society of Mechanical Engineers (ASME) Turbo Expo 2006, Power for Land, Sea, and Air, the Barcelona, Spain. May 8-11. Available at: http://www.137.205.176.10/content/ engine/ sp2-ames-turbo-2006-alexious.pdf

Azovtsev A. and Barkov A. 1988. Development of Condition Diagnostics in Russia Using Vibration. Available at: http://www.vibroket.com/articles/ russia/index.htm

Aretakis N. Mathioudakis K. and Yfantis E. A. 2008. A Possibility for Onboard Training for Marine Gas Turbine Performance. Available at: http//www.sc.iitb.ac.in /thesis/mtech2002/02323403.pdf.

2001. Afam Gas Turbine Design and Manual (Agtdm), Siemens AG Commissioning Booklet, Germany.

Baker W. E. 1991. Similarity Methods in Engineering Dynamics: Theory and Practice of Scale Modeling (Revised Edition), ISBN: 0-444-88156-5, Elsevier Science Publishers B.V, Amsterdam, The Netherlands. pp. 7-18.

Bergman J. M., Boot P. and Woud J. K. 1993. Condition Monitoring of Diesel Engines with Component Models. Paper 17, International Conference on Marine Environment and Safety (ICMES) 93, Marine Management (Holdings) Limited, the Netherland.

Cohen H. Rogers G. F. C. Saravanamutto H. I. H. 1998. Gas Turbine Theory. Longman, London. pp. 55-56.

Klaus B. and Rainer K. 2000. Introduction to Gas Turbine Theory. Solar Turbines Incorporated 2nd ed. San Diego California. pp. 22-28.

Kurzke J. 2002. Performance Modeling Methodology; Efficiency Definitions for Cooled Single and Multistage Turbines. ASME, GT-2002-20497.

Nag P. K. 2005. Power Plant Engineering. 2nd edition. McGraw Hill Publishing Co. Ltd., New Delhi, India. pp. 763-783.

Ogbonnaya E. A. 1998. Condition Monitoring of a Diesel Engine for Electricity Generation. M.Tech Thesis. Department of Marine Engineering Rivers State University of Science and Technology (RSUST), Port Harcourt. pp. 85-108.

Ogbonnaya E. A. 2004. Modeling Vibration-Based Faults in Rotor Shaft of a Gas Turbine. PhD Thesis, Dept of Mar. Engrg., RSUST, Port Harcourt, Nigeria. pp. 49-79.

Stanatis A., Mathioudakis K., Ruiz J. and Curnock B. 2001. Real Time Engine Model Implementation for Adaptive Control and Performance Monitoring of Large Civil Turbofans. *ASME* 2001-GT-362. Available at: http://www.ase.arc. nasa.gov/projects/ishem/paper/vdponi_ac_prop.doc.

APPENDIX-1

Engine characteristics

Length of rotor shaft

Compressor shaft = 1308mm
Turbine shaft = 1990mm
Generator shaft = 1080.4mm

Mass of rotors

Compressor rotor weight = 61,190N (6,240 kg)
Turbine rotor weight = 6234 kg
Area of rotor shaft 36.08m
Density, ρ = 7850 kg/m^3
(76850N/m^2)

Diameter of turbine rotor

No. 1 bearing = 215mm
No. 2 bearing = 190mm
Compressor inlet temperature (ambient) = 31^{o}C
Pressure loss at turbine output = 11.4 bar
Normal power output = 138.3MW
Fuel is natural gas
Lower heating value LHV = 44950 KJ/Kg
Fuel consumption (flow rate) = 9.3kg/s
Exhaust gas flow rate = 477kg/s
Exhaust gas temperature = 553^o C
Exhaust gas enthalpy = 610 KJ/kg